Cell Mol Neurobiol (2013) 33:99–109
DOI 10.1007/s10571-012-9875-6

ORIGINAL RESEARCH

The Reverse Roles of Transient Receptor Potential Canonical Channel-3 and -6 in Neuronal Death Following Pilocarpine-Induced Status Epilepticus

Duk-Soo Kim · Hea Jin Ryu · Ji-Eun Kim · Tae-Cheon Kang

Received: 18 July 2012 / Accepted: 14 August 2012 / Published online: 28 August 2012

Abstract Transient receptor potential canonical channel (TRPC) is a nonselective cation channel permeable to Ca^{2+}, which is expressed in many cell types, including neurons. However, the alterations in TRPC receptor expressions in response to status epilepticus (SE) have not been explored. Therefore, the present study was designated to elucidate the roles of TRPC3 and TRPC6 in neuronal death following SE. In non-SE animals, TRPC3 and TRPC6 immunoreactivity was abundantly detected in the dendrites of pyramidal cells and the cell bodies of dentate granule cells. Following SE, TRPC3 expression was significantly elevated in CA1-, CA3 pyramidal cells, and dentate granule cells, while TRPC6 expression was reduced in these regions. Pyrazole-3 (a TRPC3 inhibitor) effectively prevented up-regulation of neuronal TRPC3 expression induced by SE. Hyperforin (a TRPC6 activator) effectively prevented down-regulation of neuronal TRPC6 expression induced by SE. In addition, both Pyr3 and hyperforin effectively protected neuronal damages from SE. Therefore, the present study yields novel information regarding the role of TRPC3 and 6 in epileptogenic insults and suggests that TRPC 3 and 6 may be involved in neurodegeneration following SE.

Keywords Status epilepticus · TRPC3 · TRPC6 · Pyr3 · Hyperforin · Neuronal damage

D.-S. Kim
Department of Anatomy, College of Medicine, Soonchunhyang University, Cheonan, Chungcheongnam-Do 330-090, South Korea

H. J. Ryu · J.-E. Kim · T.-C. Kang (✉)
Department of Anatomy & Neurobiology, College of Medicine, Hallym University, Chunchon 200-702, South Korea
e-mail: tckang@hallym.ac.kr

Introduction

Status epilepticus (SE) is a medical emergency with significant mortality (DeLorenzo et al. 1995). Status epilepticus has been defined as a continuous seizure activity involving severe and prolonged hypoxia, enough to induce a sustained encephalopathy (Rossetti et al. 2007). Therefore, SE causes neuronal cell death (Fujikawa 1995; Rice and DeLorenzo 1998), epileptogenesis (Rice and DeLorenzo 1998), and learning impairment (Stewart and Persinger 2001). Pilocarpine (PILO) acts on muscarinic receptors; both M1 and M2 receptors appear to be involved. M2 receptor activation results in the inhibition of adenylate cyclase, decreasing the release of acetylcholine and neuronal excitation (Smolders et al. 1997). However, M1 receptor activation induces synthesis of phospholipase C producing diacylglycerol (DAG), and inositol-1,4,5 triphosphate (IP3), in turn, increases intracellular Ca^{2+} release (ICR) from endoplasmic reticulum via IP3 receptor and ryanodine receptors (Kim and Kang 2011).

Transient receptor potential canonical channel (TRPC) is a nonselective cation channel permeable to Ca^{2+}, which is expressed in many cell types, including neurons (Wes et al. 1995; Zhu et al. 1995; Montell et al. 2002; Harteneck et al. 2000). The TRPC subfamily is divided into seven subgroups based on their sequence similarity (Clapham 2003; Vazquez et al. 2004). The TRPC subfamily has different roles, including growth cone guidance (Li et al. 2005), neurite outgrowth (Greka et al. 2003), and neuronal survival (Jia et al. 2007). In particular, the TRPC6 protein in neurons was specifically down-regulated by the N-Methyl-D-aspartic acid (NMDA) receptor-dependent calpain proteolysis in ischemic insults. Blocking its degradation protected neurons and brains against cerebral ischemia (Du et al. 2010). Thus, TRPC6 plays a critical role in promoting neuronal survival

against NMDA receptor-mediated neuronal death (Du et al. 2010). Interestingly, the TRPC is organized into supramolecular signaling complexes, including intracellular receptors, such as IP3, ryanodine receptors, and adaptor proteins in native tissues (Kiselyov et al. 1999; Lepage et al. 2006; Redondo et al. 2004; Rosado et al. 2005; Lee et al. 2006). Among them, TRPC3 and TRPC6 are directly activated by DAG analogs (Beech et al. 2009), indicating that PILO might activate TRPC. However, the alterations in TRPC expression in response to M1 receptor-mediated SE have not been explored. Therefore, the present study was designated to elucidate the roles of TRPC3 and TRPC6 in neuronal death following SE induced by PILO.

Experimental Procedures

Experimental Animals and Chemicals

This study utilized the progeny of male Sprague–Dawley (SD) rats (7 weeks old) obtained from Experimental Animal Center, Hallym University, Chunchon, South Korea. The animals were provided with a commercial diet and water ad libitum under controlled temperature, humidity, and lighting conditions (22 ± 2 °C, 55 ± 5 %, and a 12:12 light/dark cycle with lights). Procedures involving animals and their care were conducted in accordance with our institutional guidelines that comply with NIH Guide for the Care and Use of Laboratory Animals (NIH Publications No. 80-23, 1996). In addition, all possible efforts were taken to avoid animals' suffering and to minimize the number of animals used at each stage of the experiment. All reagents were obtained from Sigma-Aldrich (St. Louis, MO, USA), except as noted.

SE Induction

In order to examine the effect of SE on TRPC3 and TRPC6 expression in the hippocampus, animals were given LiCl (3 mEq/kg i.p) 24 h before the PILO treatment. Some animals were intraperitoneally (i.p) treated with pilocarpine (30 mg/kg, i.p., Sigma, St. Louis, MO) 20 min after atropine methylbromide (5 mg/kg i.p.) and were placed in individual observation chambers where seizure activity was scored according to the system of Racine 1972). Animals that entered SE typically did so within 20 to 30 min of the administration of pilocarpine and exhibited continuous seizure activity between 2 and 5 on the Racine scale (including akinesia, facial automatisms, limbic seizures consisting of forelimb clonus with rearing, salivation, masticatory jaw movements, and falling). Diazepam (Valium, Hoffman Ia Roche, Neuilly sur-Seine, France; 10 mg/kg i.p.) was administered 2 h after the onset of SE and repeated, as needed. Age-matched animals ($n = 5$) were used as non-SE experienced controls. Non-SE animals received saline in place of PILO.

Intracerebroventricular Drug Infusion

In order to investigate the direct roles of TRPC3 and TRPC6 in SE-induced neuronal death, we performed intracerebroventricular infusion of pyrazole-3 (Pyr3, a TRPC3 receptor inhibitor) and hyperforin (TRPC6 receptor activator) prior to SE induction. The other rats were divided into three groups ($n = 6$, respectively): vehicle (0.001 % DMSO/saline, v/v), Pyr3 (0.1 mg/kg /day), and hyperforin (6 μM) treated animals. The dosage of each compound was determined as the highest dose that did not affect seizure threshold in the preliminary study. Animals were anesthetized (Zolretil, 50 mg/kg, i.m.; Virbac Laboratories) and placed in a stereotaxic frame. For the osmotic pump implantation, holes were drilled through the skull for introducing a brain infusion kit 1 (Alzet, Cupertino, CA, USA) into the right lateral ventricle (1 mm posterior; 1.5 mm lateral; −3.5 mm depth; flat skull position with bregma as reference), according to the atlas of the rat brain (Paxinos and Watson 1997). The infusion kit was sealed with dental cement and connected to an osmotic pump (1007D, Alzet, Cupertino, CA, USA). The pump was placed in a subcutaneous pocket in the dorsal region. Animals received 0.5 μl/hr of vehicle or compound for 1 week (Siuciak et al. 1996; Pencea et al. 2001; Kim et al. 2010). Three days after surgery, rats were induced with SE using the same methods described above. Rest of the animals ($n = 3$ in each group) were used as non-SE experienced controls. Since neuronal damage was first detectable at 3 days after SE (Kang et al. 2006), we determined 3 days after SE as the best time point to evaluate the effects of Pyr3 and hyperforin infusion on SE-induced neuronal damages. Therefore, these animals were stained with fluoro-Jade B (FJB) and double immunofluorescence study was conducted 3 days after SE using the methods described below.

Tissue Processing

At the designated time points (Non-SE, 1 day, 3 days, and 1 week after SE, $n = 5$, respectively), animals were perfused transcardially with phosphate-buffered saline (PBS, pH 7.4) followed by 4 % paraformaldehyde in 0.1 M phosphate buffer (PB, pH 7.4) under urethane anesthesia (1.5 g/kg i.p.). Drug-infused animals were perfused using the same methods, 3 days after SE. The brains were removed, postfixed in the same fixative for 4 h, and rinsed in PB containing 30 % sucrose at 4 °C for 2 days. Thereafter, the tissues were frozen and sectioned with a cryostat at 30 μm.

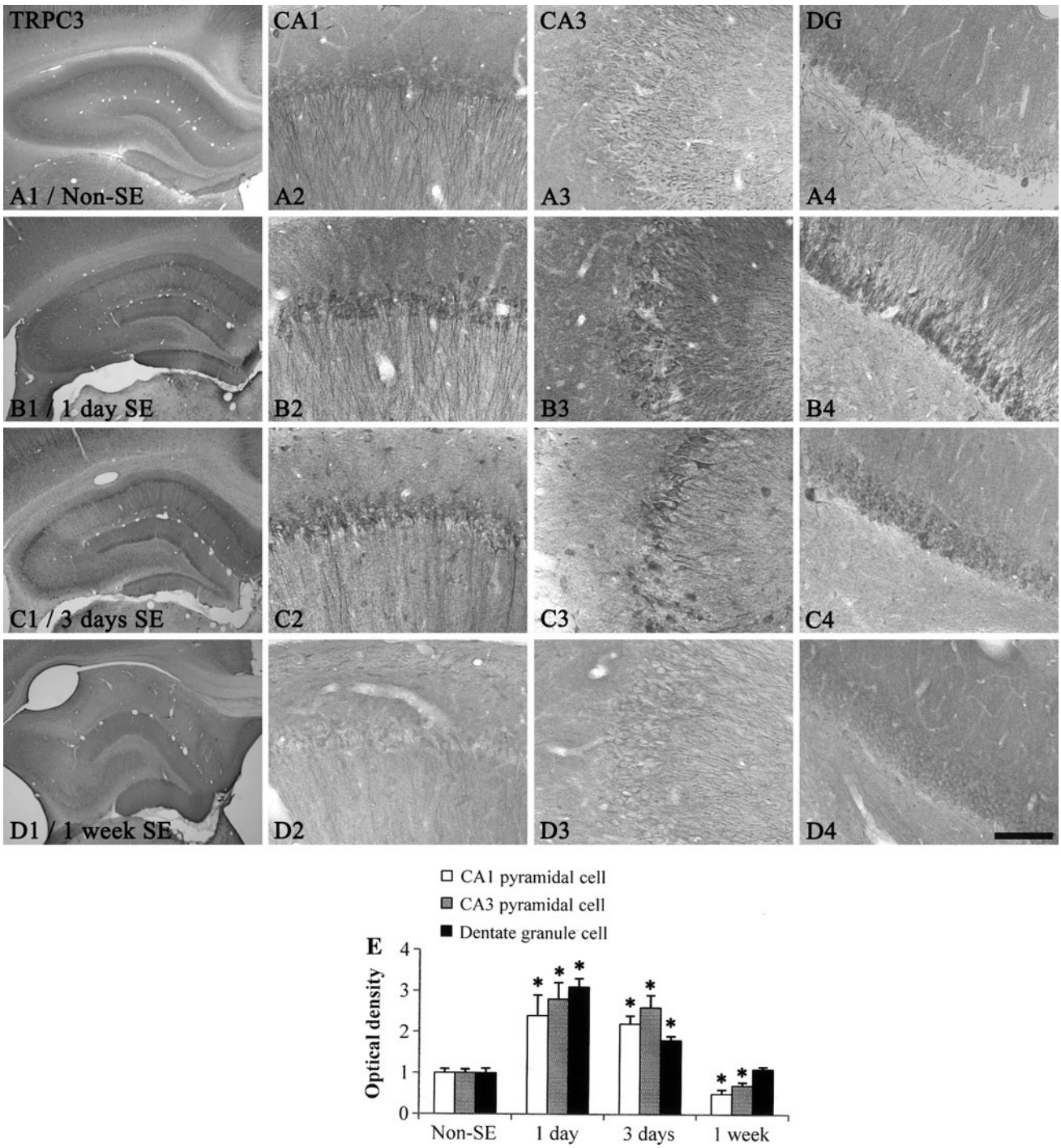

Fig. 1 TRPC3 expression in the hippocampus following SE. **a** Non-SE animal. *Bar* = 400 (*panel 1*) and 50 μm (*panel 2–4*). **b** One day-post SE animals. *Bar* = 400 (*panel 1*) and 50 μm (*panel 2–4*). **c** Three days-post SE animals. *Bar* = 400 (*panel 1*) and 50 μm (*panel 2–4*). **d** One week-post SE animals. *Bar* = 400 (*panel 1*) and 50 μm (*panel 2–4*). **e** Quantitative analysis of TRPC3 expression in the hippocampus following SE (mean ± SEM). Significant differences from vehicle-treated groups (*$p < 0.05$ vs. non-SE animals). *DG* dentate granule cell layer; *CA1* pyramidal cell layer; *CA3* pyramidal cell layer

FJB Staining

Fluoro-Jade B (FJB) staining was used to identify degenerating neurons in tissues obtained from non-SE and 3-days-post-SE animals in drug-infused groups. In brief, the brain sections were rinsed in distilled water, mounted onto gelatin-coated slides, and then dried on a slide warmer. The slides were immersed in 100 % ethanol for

3 min, followed by 70 % ethanol for 2 min and distilled water for 2 min. The slides were then transferred to 0.06 % potassium permanganate for 15 min and gently agitated. After rinsing in distilled water for 2 min, the slides were incubated for 30 min in 0.001 % FJB (Histo-Chem Inc. Jefferson, AR, USA), freshly prepared by adding 20 ml of a 0.01 % stock FJB solution to 180 ml of 0.1 % acetic acid, with gentle shaking in the dark. After rinsing for 1 min in each of three changes of distilled water, the slides were dried, dehydrated in xylene, and coverslipped with DPX.

Immunohistochemistry

In each animal, the free-floating sections were first incubated with 10 % normal chicken serum (Vector, Burlingame, CA, USA) for 30 min at room temperature. Some sections were incubated in either of the following antibodies : rabbit anti-TRPC3 (diluted 1:200, Alomone labs, Jerusalem, Israel) or TRPC6 antibody (diluted 1:200, Millipore Corporation, Billerica, MA, USA) in PBS containing 0.3 % Triton X-100 and 2 % normal chicken serum (Vector, Burlingame, CA, USA) overnight at room temperature. After washing three times for 10 min with PBS, the sections were incubated sequentially in donkey anti-rabbit IgG (Vector, Burlingame, CA, USA) and ABC complex (Vector, Burlingame, CA, USA), diluted 1:200 in the same solution as the primary antiserum. Between the incubations, the tissues were washed with PBS three times for 10 mins each. The sections were visualized with 3,3′-diaminobenzidine in 0.1 M Tris buffer and mounted on the gelatin-coated slides. The immunoreactions were observed under the Axioscope microscope (Carl Zeiss, Munchen-Hallbergmoos, Germany).

For double immunofluorescence study, some sections were incubated in either mixture of antibodies: rabbit anti-TRPC3 (diluted 1:100) or TRPC6 antibody (diluted 1:100)/ mouse anti-neuronal nuclear antigen (NeuN) antibody (a neuronal marker, Millipore Corporation, Billerica, MA, USA, diluted 1:1,000) in PBS containing 0.3 % Triton X-100 overnight at room temperature. After washing three times for 10 min with PBS, the sections were also incubated in a mixture of fluorescein isothio-cyanate-conjugated secondary antiserum and Cy3-conjugated secondary antiserum (diluted 1:200, Amersham, San Francisco, CA, USA) for 1 h at room temperature. The sections were washed three times for 10 min with PBS and mounted on gelatin-coated slides. For nuclei counterstaining, we used Vectashield mounting medium with DAPI (Vector, Burlingame, CA, USA). For negative control, the rat hippocampal tissues were incubated with 1 μg of the antibody that was preincubated with 1 μg of purified peptide for 1 h at room temperature (for TRPC3 and TRPC6), or incubated with pre-immune serum instead of primary antibody (for NeuN). The negative control resulted in the absence of immunoreactivity in any of the structures.

Fig. 2 Effect of TRPC3 inhibitor (Pyr3) on neuronal death in the hippocampus following SE. **a**, **b** Non-SE animals; **c**, **d** three days-post SE animals treated with vehicle; **e**, **f** three days-post SE animals treated with Pyr-3. **b**, **d**, **f** High magnification of CA1 pyramidal cells. *Panels 1, 2, 3*, and *4* are TRPC3, NeuN, DAPI counterstaining, and merge images, respectively. *Bar* = 400 (**a**, **c**, **e**) and 12.5 μm (**b**, **d**, **f**). **g** Quantitative analysis of TRPC3 expression in the hippocampus following SE (mean ± SEM). Significant differences from non-SE animals and vehicle-treated animals (* and # $p < 0.05$ vs. non-SE animals and vehicle-treated animals, respectively) ▶

All images were captured using an Axiocam HRc camera and Axio Vision 3.1 software.

Stereology

The hippocampal volumes (V) were estimated according to the formula based on the modified Cavalieri method: $V = \Sigma a \times t_{nom} \times 1/ssf$, where a is area of the region of the delineated subfield measured by AxioVision Rel. 4.8 software, t_{nom} is the nominal section thickness (of 30 μm in this study), and ssf is the fraction of the sections sampled or section sampling fraction (of 1/6 in this study). The subfield areas were delineated with a 2.5 × objective lens. The volumes are reported as mm^3 (Bedi et al. 1991; Madeira et al. 1995). The optical fractionator was used to estimate the cell numbers. The optical fractionator (combination of performing counting with the optical dissector, with fractionator sampling) is a stereological method based on a properly designed systematic random sampling method that, by definition, yields unbiased estimates of population number. The sampling procedure is accomplished by focusing through the depth of the tissue (the optical dissector height, h, of 15 μm in all cases for this study). The number of each cell type (C) in each of the subregions is estimated as: $C = \Sigma Q^{-} \times t/h \times 1/asf \times 1/ssf$, where Q^{-} is the number of cells actually counted in the dissectors that fell within the sectional profiles of the subregion seen on the sampled sections, and asf is the area sampling fraction calculated by the area of the counting frame of the dissector, a(frame) (of 50 × 50 $\mu\mathrm{m}^2$ in this study) and the area associated with each x, y movement, grid (x, y step) (of 250 × 250 $\mu\mathrm{m}^2$ in this study) $\{\mathrm{asf} = [a(\mathrm{frame})/a(x, y\,\mathrm{step})]\}$. Fluoro-Jade B (FJB) positive cells were counted with a 40× objective lens. All FJB positive cells were counted regardless of the intensity of labeling. Cell counts were performed by two different investigators who were blind to the classification of tissues. The SE-induced hippocampal atrophy is evident (Niessen et al. 2005; Roch et al. 2002), so changes in cell number may be caused by an alteration in the volume of the hippocampus. Therefore, the total number of cells was corrected by multiplying with appropriate correction factors representing the degree of shrinkage (or swelling) compared with the non-SE animals (Kim et al. 2011a).

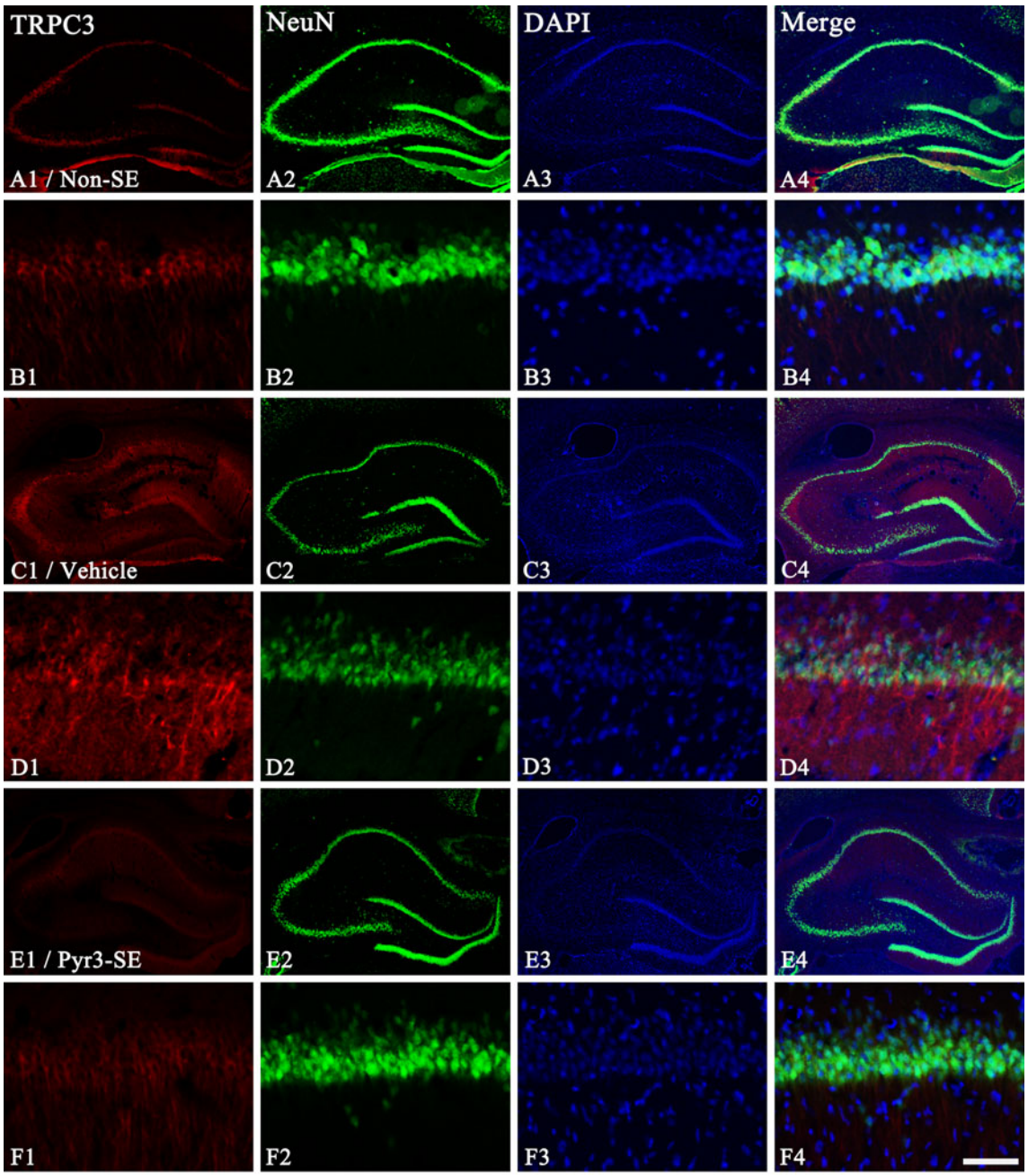
TRPC3
NeuN
DAPI
Merge
A1 / Non-SE
A2
A3
A4
B1
B2
B3
B4
C1 / Vehicle
C2
C3
C4
D1
D2
D3
D4
E1 / Pyr3-SE
E2
E3
E4
F1
F2
F3
F4

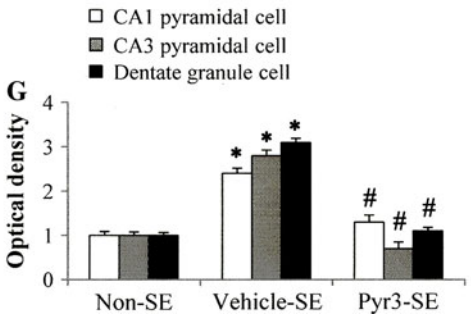
CA1 pyramidal cell
CA3 pyramidal cell
Dentate granule cell
G
Optical density
0
1
2
3
4
*
*
*
#
#
#
Non-SE
Vehicle-SE
Pyr3-SE

Quantification of Data and Statistical Analysis

For quantification of immunohistochemical data, images were captured using an AxioImage M2 microscope and AxioVision Rel. 4.8 software (15 sections per animal). Figures were mounted with Adobe PhotoShop v 8.0. Images were converted into gray and white images. The range of intensity values was obtained from the selected images using Adobe PhotoShop v. 8.0. Based on the mean range of intensity values, each image was normalized by adjusting the black and white range of the image using Adobe PhotoShop v. 8.0. Manipulation of the images was restricted to threshold and brightness adjustments to the whole image. After regions were outlined, 10 areas/rat (500 μm^2/area) were selected from the hippocampus and the gray values were measured. Intensity measurements were represented as the mean number of a 256 gray scale (NIH Image 1.59 software and AxioVision Rel. 4.8 software). Values for background staining were obtained from the corpus callosum. Optical density values were then corrected by subtracting the average values of background noise obtained from 15 image inputs. All data obtained from the quantitative measurements were analyzed using one-way analysis of variance to determine statistical significance. Bonferroni's test was used for post hoc comparisons. A p value below 0.05 was considered statistically significant (Kim et al. 2009a– c).

Results

Up-regulation of Neuronal TRPC3 Expression Following SE

In non-SE animals (Figs. 1a, 2a, b), TRPC3 immunoreactivity was abundantly detected in the dendrites of pyramidal cells and the cell bodies of dentate granule cells. One day after SE (Fig. 1b, e), elevated TRPC3 immunoreactivity was observed only in NeuN positive neurons. Transient receptor potential canonical channel 3 (TRPC3) immunoreactivity was obviously detected in the dendrites of pyramidal cells and dentate granule cells. Transient receptor potential canonical channel 3 (TRPC3) expression in CA1-, CA3-pyramidal cells, and dentate granule cells was increased to 2.4, 2.8, and 3.1-fold of the non-SE level, respectively ($p < 0.05$ vs. non-SE, $n = 5$, respectively). Three days after SE (Fig. 1c, e), elevated TRPC3 expression was maintained in CA1-, CA3- and dentate granule cells. One week after SE (Fig. 1d, e), TRPC3 expression in CA1- and CA3- pyramidal cells was reduced to 0.5 and 0.7-fold of the non-SE level, respectively ($p < 0.05$ vs. non-SE, $n = 5$, respectively), due to massive neuronal death. However, TRPC3 expression in dentate granule cells was similar to that observed in non-SE animals. Pyrazole-3 pretreatment effectively prevented up-regulation of neuronal TRPC3 expression induced by SE ($p < 0.05$ vs. vehicle, $n = 3$, respectively, Fig. 2).

Down-regulation of Neuronal TRPC6 Expression Following SE

In non-SE animals (Figs. 3a, 4a, b), TRPC6 immunoreactivity was mainly detected in the dendrites of pyramidal cells and the cell bodies of dentate granule cells. In addition, TRPC6 immunoreactivity was also strongly observed in neuropils within the molecular layer of the dentate gyrus. One day after SE (Fig. 3b, e), TRPC6 expression in CA1-, CA3- pyramidal cells and dentate granule cells was reduced to 0.51, 0.48, and 0.52-fold of the non-SE level, respectively ($p < 0.05$ vs. non-SE, $n = 5$, respectively). In addition, reduced TRPC6 immunoreactivity was detected in the inner molecular layer of the dentate gyrus. Three days after SE (Figs. 3c, e, 4c, d), TRPC6 expression was unaltered in the hippocampus except the molecular layer of the dentate gyrus where TRPC6 expression was reduced to 0.3-fold of the non-SE level ($p < 0.05$ vs. non-SE), as compared to 1 day-post-SE animals ($n = 5$, respectively). Following SE, TRPC6 expression was also detected in astrocytes in the CA1 subfield of the hippocampus proper following SE (data not shown). One week after SE (Fig. 3d, e), TRPC6 expression in CA1-, CA3- pyramidal cells, and dentate granule cells was reduced to 0.21-, 0.31-, and 0.18-fold of the non-SE level, respectively ($p < 0.05$ vs. non-SE, $n = 5$, respectively). Hyperforin pretreatment effectively prevented down-regulation of neuronal TRPC6 expression induced by SE ($p < 0.05$ vs. vehicle, $n = 3$, respectively, Fig. 4).

Neuronal Damages

In our previous (Ryu et al. 2011) and preliminary data, neuronal damage was first detectable 3 days after SE. Therefore, we applied FJB stains in 3 days-post SE animals that were pretreated with vehicle, Pyr3, and hyperforin. Few FJB positive neurons were detected in the hippocampus of non-SE induced animals of all groups (data not shown). In vehicle-treated animals, FJB positive neurons were detected in CA1-3 pyramidal cells and dentate hilus neurons (Fig. 5a). The number of FJB positive neurons in the dentate hilus, the CA1, and the CA3 region was 16,102 ± 4,325, 262,038 ± 48,174, and 298,681 ± 15,269, respectively (Fig. 5d, f). As compared to vehicle-treated animals, Pyr3- or hyperforin-treated animals showed significant reductions in neuronal damages induced by SE within the hippocampus ($p < 0.05$ vs. vehicle, $n = 3$, respectively): In Pyr3-pretreated animals, the number of FJB positive neurons in the dentate hilus, the CA1, and the CA3 region was significantly reduced to 4,601 ± 1,272, 72,788 ± 8,352, and 123,141 ± 13,983, respectively

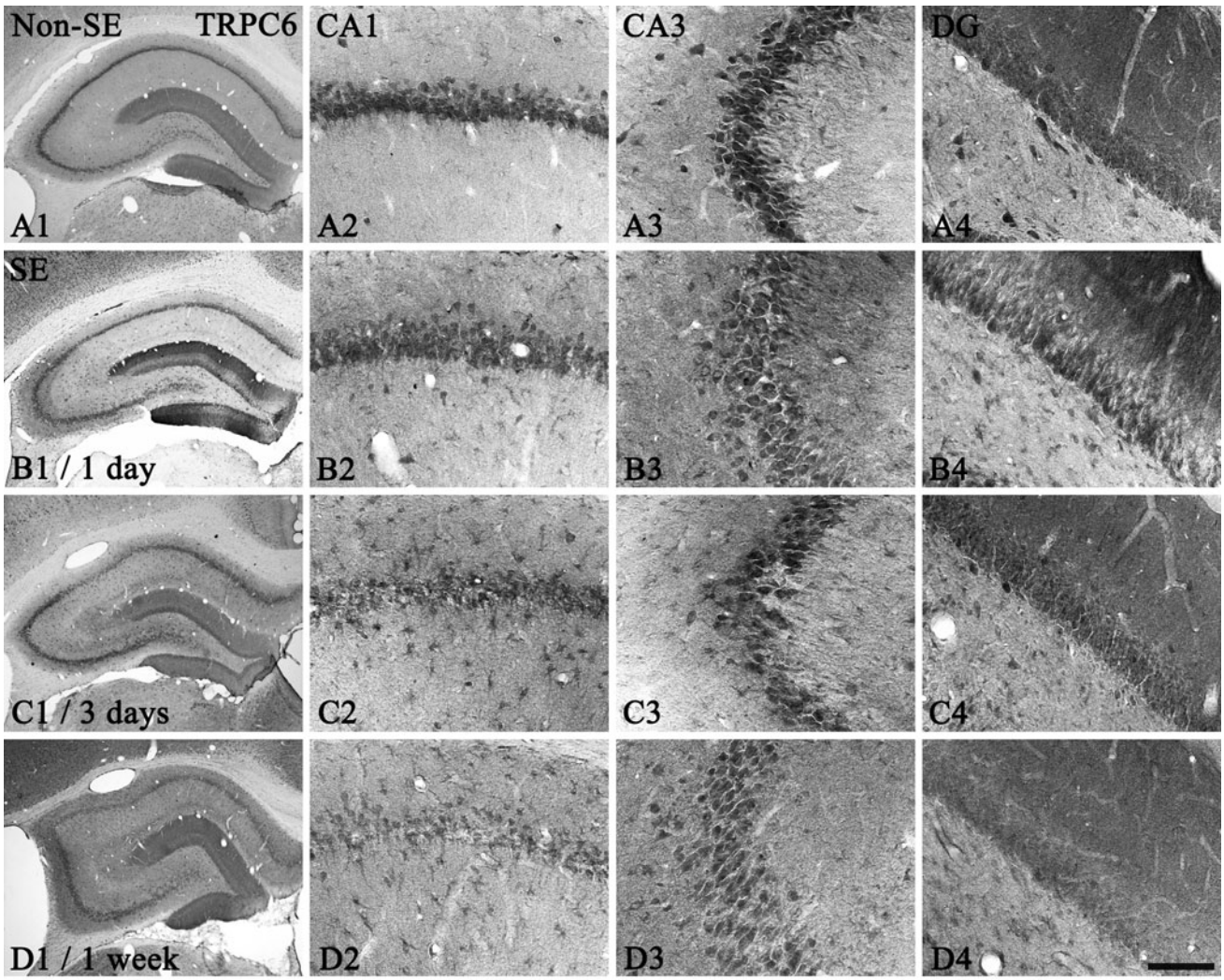

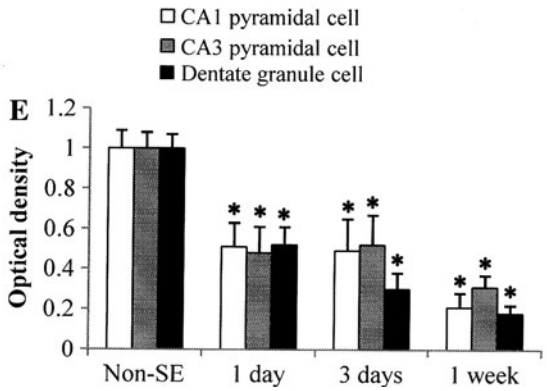

Fig. 3 TRPC6 expression in the hippocampus following SE. **a** Non-SE animal. *Bar* = 400 (*panel 1*) and 50 μm (*panel 2–4*). **b** One day-post SE animals. *Bar* = 400 (*panel 1*) and 50 μm (*panel 2–4*). **c** Three days-post SE animals. *Bar* = 400 (*panel 1*) and 50 μm (*panel 2–4*). **d** One week-post SE animals. *Bar* = 400 (*panel 1*) and 50 μm (*panel 2–4*). **e** Quantitative analysis of TRPC6 expression in the hippocampus following SE (mean ± SEM). Significant differences from vehicle-treated groups (*$p < 0.05$ vs. non-SE animals). *DG* dentate granule cell layer; *CA1* pyramidal cell layer; *CA3* pyramidal cell layer

(Fig. 5b, d–f). In hyperforin-pretreated animals, the number of FJB positive neurons in the dentate hilus, the CA1, and the CA3 region was significantly reduced to 5,367 ± 1,364, 87,312 ± 6,312, and 103,108 ± 12,038, respectively (Fig. 5c–f). These findings indicate reverse roles of TRPC3 and TRPC6 in SE-induced neuronal death.

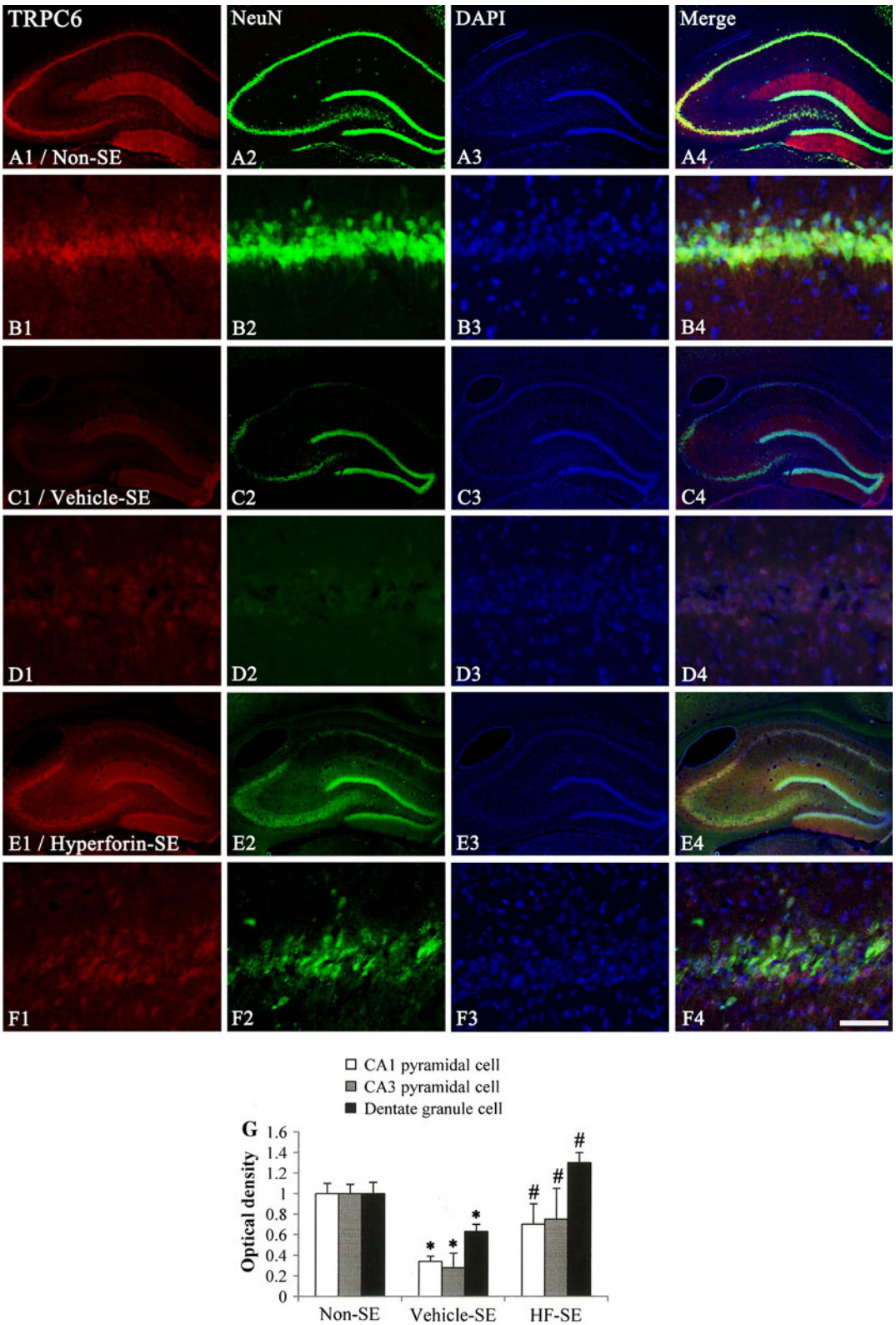

Fig. 4 Effect of TRPC6 activator (hyperforin) on neuronal death in the hippocampus following SE. **a**, **b** Non-SE animals; **c**, **d** three days-post SE animals treated with vehicle; **e**, **f** three days-post SE animals treated with hyperforin. **b**, **d**, **f** High magnification of CA1 pyramidal cells. *Panels 1, 2, 3, and 4* are TRPC3, NeuN, DAPI counterstaining, and merge images, respectively. *Bar* = 400 (**a**, **c**, **e**) and 12.5 μm (**b**, **d**, **f**). **g** Quantitative analysis of TRPC6 expression in the hippocampus following SE (mean ± SEM). Significant differences from non-SE animals and vehicle-treated animals (* and # $p < 0.05$ vs. non-SE animals and vehicle-treated animals, respectively)

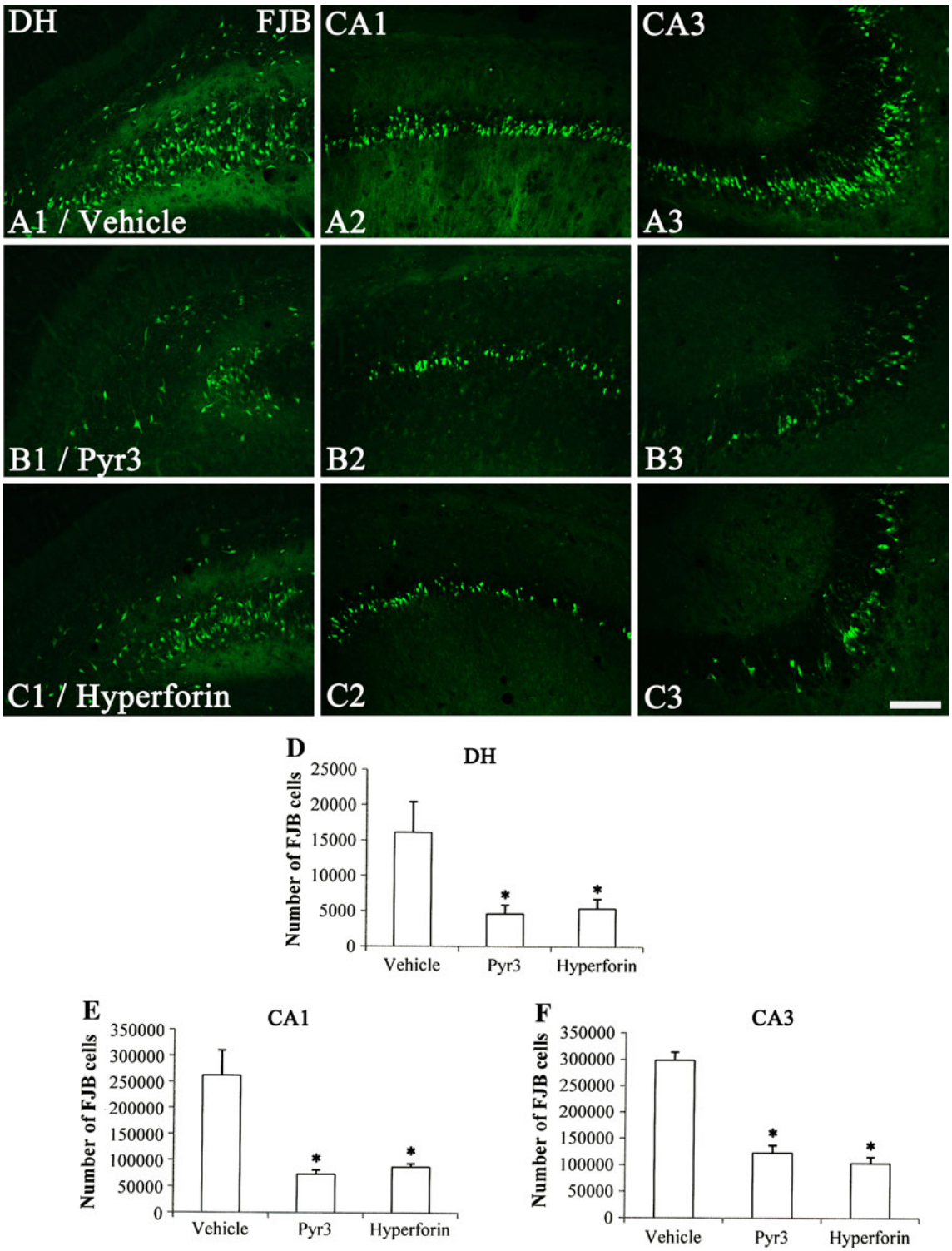

Fig. 5 Effects of Pyr3 and hyperforin on neuronal damages in the hippocampus following SE. **a** Vehicle-treated animals; **b** pyr3-treated animals; **c** hyperforin-treated animals. *Bar* = 20 μm. (**d–f**) Quantitative analysis of FJB positive neurons in the hippocampus following SE (mean ± SEM). Significant differences from vehicle-treated animals (*$p < 0.05$ vs. non-SE animals). *DH* dentate hilar cell; *CA1* pyramidal cell; *CA3* pyramidal cell

Discussion

In epileptic hippocampus, severe neurodegeneration occurs both in principal neurons and in interneurons (Mathern et al. 1995; Wittner et al. 2001). Neurodegeneration in the hippocampus is not uniform, but heterogeneous among the principal hippocampal cell layers. For example, dentate granule cells are remarkably resistant to neuronal damage caused by SE. Conversely, dentate hilar neurons, CA1-, and CA3- pyramidal neurons are extremely vulnerable to SE (Kim et al. 2011b; Ryu et al. 2011). Malfunction of muscarinic acetylcholine receptor transmission is one of the candidates for the prolonged depolarization underlying seizure-related neuronal death (Kim et al. 2011b; Kim and Kang 2011). Recently, TRPC functions are activated by the formation of DAG and IP_3, followed by activation of IP_3 receptors in intracellular Ca^{2+} stores (Clapham 2003; Montell et al. 2002). Therefore, it is likely that TRPC may participate in the regulation of muscarinic receptor-mediated neuronal death. Indeed, the present study showed that TRPC6 expression was reduced in CA1-3 neurons as well as dentate granule cells. Furthermore, hyperforin pretreatment effectively protected neuronal death from SE insults. These findings are consistent that TRPC6 function is suppressed in ischemia and the maintenance of TRPC6 expression is neuroprotective via the cAMP response element-binding-dependent mechanism (Du et al. 2010). Thus, our findings suggest that activation of TRPC6 function or inhibition of TRPC6 degradation may protect neuronal damages from SE, like ischemic brain damage.

In the present study, TRPC3 expression was significantly elevated in the hippocampus following SE. Since TRPC3 mRNA expression is increased in TRPC6 knockout mice (Tiruppathi et al. 2002), it is likely that increase in TRPC3 expression induced by SE may be a compensatory mechanism for reduction in TRPC6 function. However, TRPC3 and TRPC6 are not functionally interchangeable (Carrillo et al. 2012; Urban et al. 2012; Cheung et al. 2011). Furthermore, the present study showed that up-regulated TRPC3 expression may not be correlated with altered TRPC6 expression and that the inhibition of TRPC3 function by Pyr3 effectively prevented SE-induced neuronal death. On the other hand, TRPC3 is needed to activate a nonselective cationic current by brain-derived neurotrophic factor (BDNF) (Amaral and Pozzo-Miller 2007), which can facilitate and potentially initiate seizure activity (Scharfman et al. 2002). Blockade of BDNF function effectively decreases SE-induced neuronal death, indicating an injury-facilitating role for BDNF in vivo (Unsain et al. 2009). Based on these previous studies, it is likely that up-regulated TRPC3 expression may be involved in the BDNF-mediated neuronal death following SE. Further studies are needed to elucidate the role of TRPC3 in neuronal death.

In conclusion, the present study yields novel information regarding the role of TRPC3 and 6 in epileptogenic insults, and suggest that TRPC 3 and 6 may be involved in neurodegeneration following SE.

Acknowledgments This work was supported by the National Research Foundation of Korea (NRF) grant funded by the Korea government (MEST) (No. 2012R1A2A1A01001775 and 2009-0093812) and Hallym University (HRF-201206-007).

References

Amaral MD, Pozzo-Miller L (2007) BDNF induces calcium elevations associated with IBDNF, a nonselective cationic current mediated by TRPC channels. J Neurophysiol 98:2476–2482

Bedi KS (1991) Early-life undernutrition causes deficits in rat dentate gyrus granule cell number. Experientia 47:1073–1074

Beech DJ, Bahnasi YM, Dedman AM, Al-Shawaf E (2009) TRPC channel lipid specificity and mechanisms of lipid regulation. Cell Calcium 45:583–588

Carrillo C, Hichami A, Andreoletti P, Cherkaoui-Malki M, Del Mar Carvia M, Abdoul-Azize S, Alonso-Torre SR, Khan NA (2012) Diacylglycerol-containing oleic acid induces increases in $[Ca(^{2+})](i)$ via TRPC3/6 channels in human T cells. Biochim Biophys Acta 1821:618–626

Cheung KK, Yeung SS, Au SW, Lam LS, Dai ZQ, Li YH, Yeung EW (2011) Expression and association of TRPC1 with TRPC3 during skeletal myogenesis. Muscle Nerve 44:358–365

Clapham DE (2003) TRP channels as cellular sensors. Nature 426: 517–524

DeLorenzo RJ, Pellock JM, Towne AR, Boggs JG (1995) Epidemiology of status epilepticus. J Clin Neurophysiol 12:316–325

Du W, Huang J, Yao H, Zhou K, Duan B, Wang Y (2010) Inhibition of TRPC6 degradation suppresses ischemic brain damage in rats. J Clin Invest 120:3480–3492

Fujikawa DG (1995) Neuroprotective effect of ketamine administered after status epilepticus onset. Epilepsia 36:186–195

Greka A, Navarro B, Oancea E, Duggan A, Clapham DE (2003) TRPC5 is a regulator of hippocampal neurite length and growth cone morphology. Nat Neurosci 6:837–845

Harteneck C, Plant TD, Schultz G (2000) From worm to man: three subfamilies of TRP channels. Trends Neurosci 23:159–166

Jia Y, Zhou J, Tai Y, Wang Y (2007) TRPC channels promote cerebellar granule neuron survival. Nat Neurosci 10:559–567

Kang TC, Kim DS, Kwak SE, Kim JE, Won MH, Kim DW, Choi SY, Kwon OS (2006) Epileptogenic roles of astroglial death and regeneration in the dentate gyrus of experimental temporal lobe epilepsy. Glia 54:258–271

Kim JE, Kang TC (2011) The P2X7 receptor-pannexin-1 complex decreases muscarinic acetylcholine receptor-mediated seizure susceptibility in mice. J Clin Invest 121:2037–2047

Kim JE, Kim DW, Kwak SE, Ryu HJ, Yeo SI, Kwon OS, Choi SY, Kang TC (2009a) Pyridoxal-5'-phosphate phosphatase/chronophin inhibits long-term potentiation induction in the rat dentate gyrus. Hippocampus 19:1078–1089

Kim JE, Kwak SE, Kang TC (2009b) Upregulated TWIK-related acid-sensitive K + channel-2 in neurons and perivascular astrocytes in the hippocampus of experimental temporal lobe epilepsy. Epilepsia 50:654–663

Kim JE, Ryu HJ, Yeo SI, Seo CH, Lee BC, Choi IG, Kim DS, Kang TC (2009c) Differential expressions of aquaporin subtypes in astroglia in the hippocampus of chronic epileptic rats. Neuroscience 163:781–789

Kim JE, Ryu HJ, Yeo SI, Kang TC (2010) P2X7 receptor regulates leukocyte infiltrations in rat frontoparietal cortex following status epilepticus. J Neuroinflamm 7:65

Kim JE, Ryu HJ, Yeo SI, Kang TC (2011a) P2X7 receptor differentially modulates astroglial apoptosis and clasmatodendrosis in the rat brain following status epilepticus. Hippocampus 21:1318–1333

Kim JE, Ryu HJ, Kang TC (2011b) P2X7 receptor activation ameliorates CA3 neuronal damage via a tumor necrosis factor-α-mediated pathway in the rat hippocampus following status epilepticus. J Neuroinflamm 8:62

Kiselyov K, Mignery GA, Zhu MX, Muallem S (1999) The N-terminal domain of the IP3 receptor gates store-operated hTrp3 channels. Mol Cell 4:423–429

Lee EH, Cherednichenko G, Pessah IN, Allen PD (2006) Functional coupling between TRPC3 and RyR1 regulates the expressions of key triadic proteins. J Biol Chem 281:10042–10048

Lepage PK, Lussier MP, Barajas-Martinez H, Bousquet SM, Blanchard AP, Francoeur N, Dumaine R, Boulay G (2006) Identification of two domains involved in the assembly of transient receptor potential canonical channels. J Biol Chem 281:30356–30364

Li Y, Jia YC, Cui K, Li N, Zheng ZY, Wang YZ, Yuan XB (2005) Essential role of TRPC channels in the guidance of nerve growth cones by brain-derived neurotrophic factor. Nature 434:894–898

Madeira MD, Sousa N, Santer RM, Paula-Barbosa MM, Gundersen HJ (1995) Age and sex do not affect the volume, cell numbers, or cell size of the suprachiasmatic nucleus of the rat: an unbiased stereological study. J Comp Neurol 361:585–601

Mathern GW, Babb TL, Pretorius JK, Melendez M, Lévesque MF (1995) The pathophysiologic relationships between lesion pathology, intracranial ictal EEG onsets, and hippocampal neuron losses in temporal lobe epilepsy. Epilepsy Res 21:133–147

Montell C, Birnbaumer L, Flockerzi V, Bindels RJ, Bruford EA, Caterina MJ, Clapham DE, Harteneck C, Heller S, Julius D, Kojima I, Mori Y, Penner R, Prawitt D, Scharenberg AM, Schultz G, Shimizu N, Zhu MX (2002) A unified nomenclature for the superfamily of TRP cation channels. Mol Cell 9:229–231

Niessen HG, Angenstein F, Vielhaber S, Frisch C, Kudin A, Elger CE, Heinze HJ, Scheich H, Kunz WS (2005) Volumetric magnetic resonance imaging of functionally relevant structural alterations in chronic epilepsy after pilocarpine-induced status epilepticus in rats. Epilepsia 46:1021–1026

Paxinos G, Watson C (1997) Rat brain in stereotaxic coordinates, 3rd edn. Academic Press, San Diego

Pencea V, Bingaman KD, Wiegand SJ, Luskin MB (2001) Infusion of brain-derived neurotrophic factor into the lateral ventricle of the adult rat leads to new neurons in the parenchyma of the striatum, septum, thalamus, and hypothalamus. J Neurosci 21:6706–6717

Racine RJ (1972) Modification of seizure activity by electrical stimulation. II. Motor seizure. Electroencephalogr. Clin Neurophysiol 32:281–294

Redondo PC, Harper AG, Salido GM, Pariente JA, Sage SO, Rosado JA (2004) A role for SNAP-25 but not VAMPs in store-mediated Ca^{2+}entry in human platelets. J Physiol 558:99–109

Rice AC, DeLorenzo RJ (1998) NMDA receptor activation during status epilepticus is required for the development of epilepsy. Brain Res 782:240–247

Roch C, Leroy C, Nehlig A, Namer IJ (2002) Magnetic resonance imaging in the study of the lithium-pilocarpine model of temporal lobe epilepsy in adult rats. Epilepsia 43:325–335

Rosado JA, Redondo PC, Salido GM, Sage SO, Pariente JA (2005) Cleavage of SNAP-25 and VAMP-2 impairs store-operated Ca^{2+}entry in mouse pancreatic acinar cells. Am J Physiol Cell Physiol 288:C214–C221

Rossetti AO, Logroscino G, Liaudet L, Ruffieux C, Ribordy V, Schaller MD, Despland PA, Oddo M (2007) Status epilepticus: an independent outcome predictor after cerebral anoxia. Neurology 69:255–260

Ryu HJ, Kim JE, Yeo SI, Kim MJ, Jo SM, Kang TC (2011) ReLA/P65-serine 536 nuclear factor-kappa B phosphorylation is related to vulnerability to status epilepticus in the rat hippocampus. Neuroscience 187:93–102

Scharfman HE, Goodman JH, Sollas AL, Croll SD (2002) Spontaneous limbic seizures after intrahippocampal infusion of brain-derived neurotrophic factor. Exp Neurol 174:201–214

Siuciak JA, Boylan C, Fritsche M, Altar CA, Lindsay RM (1996) BDNF increases monoaminergic activity in rat brain following intracerebroventricular or intraparenchymal administration. Brain Res 710:11–20

Smolders I, Bogaert L, Ebinger G, Michotte Y (1997) Muscarinic modulation of striatal dopamine, glutamate, and GABA release, as measured with in vivo microdialysis. J Neurochem 68:1942–1948

Stewart LS, Persinger MA (2001) Ketamine prevents learning impairment when administered immediately after status epilepticus onset. Epilepsy Behav 2:585–591

Tiruppathi C, Freichel M, Vogel SM, Paria BC, Mehta D, Flockerzi V, Malik AB (2002) Impairment of store-operated Ca^{2+}entry in TRPC4(−/−) mice interferes with increase in lung microvascular permeability. Circ Res 91:70–76

Unsain N, Montroull LE, Mascó DH (2009) Brain-derived neurotrophic factor facilitates TrkB down-regulation and neuronal injury after status epilepticus in the rat hippocampus. J Neurochem 111:428–440

Urban N, Hill K, Wang L, Kuebler WM, Schaefer M (2012) Novel pharmacological TRPC inhibitors block hypoxia-induced vasoconstriction. Cell Calcium 51:194–206

Vazquez G, Wedel BJ, Aziz O, Trebak M, Putney JW Jr (2004) The mammalian TRPC cation channels. Biochem Biophys Acta 1742:21–36

Wes PD, Chevesich J, Jeromin A, Rosenberg C, Stetten G, Montell C (1995) TRPC1, a human homolog of a *Drosophila* store-operated channel. Proc Natl Acad Sci USA 92:9652–9656

Wittner L, Maglóczky Z, Borhegyi Z, Halász P, Tóth S, Eross L, Szabó Z, Freund TF (2001) Preservation of perisomatic inhibitory input of granule cells in the epileptic human dentate gyrus. Neuroscience 108:587–600

Zhu X, Chu PB, Peyton M, Birnbaumer L (1995) Molecular cloning of a widely expressed human homolog for the *Drosophila* trp gene. FEBS Lett 373:193–198